Supporting Information

Karpowich and Wang 10.1073/pnas.1217361110

SI Materials and Methods

Identification of the ECF Transporter Subunits of *Thermotoga maritima*. The subunits of the ECF transporter from *T. maritima* were identified by sequence similarity searches in BLAST (1) using the homologous proteins from *Lactococcus lactis* as seeds: EcfA (Llmg_0288, GI: 152031905), EcfA′ (Llmg_0287, GI: 52031898), EcfT (Llmg_0289, GI: 334305761), and RibU (Llmg_1195, GI: 313471444) (2). These searches unambiguously identified TM0222, TM1663, TM1868, and TM1455 as the EcfA, A′, T, and RibU homologs, respectively.

Complementation of an *Escherichia coli* Riboflavin Auxotroph. The *E. coli* riboflavin auxotrophic strain BSV11 (3) was obtained from the *E. coli* genetic stock center at Yale University. This strain contains a mutation in the *ribB* gene, which encodes an essential enzyme in the riboflavin biosynthesis pathway. BSV11 was lysogenized with the λDE3 kit (EMD4Biosciences) to enable coexpression of TmECF genes from pET vectors. Otherwise, the assays were performed as described in ref. 4.

Expression and Purification of the ECF Riboflavin Transporter from *Streptococcus thermophilus*. The following ECF and RibU genes from *S. thermophilus* were identified by sequence homology to their *T. maritima* counterparts as *Stu2007* (T), *Stu2008* (A), *Stu2009* (A′), and *Stu0268* (RibU). A polycistronic operon was constructed by linking the genes with ribosome binding sites between them in the following order: T–RibU–A–A′ and cloned into modified pBAD vector with a carboxyl-terminal myc-deca-histidine tag linked by a thrombin recognition site. This construct was transformed into *E. coli* BL21(DE3), and protein expression was performed in LB media at 37 °C. Cells were resuspended in Buffer A. After cell disruption, unlysed cells were removed by centifugation and the membrane fraction was isolated by ultra-centfiguation. Membranes were resuspended in Buffer A and treated with 1% DDM for membrane protein solublization. The StuECF–RibU complex was bound to Talon resin in DDM and exchanged into SEC buffer (20 mM Tris, pH 7.5, 100 mM NaCl, 10% glycerol, and 0.04% DDM) by thrombin cleavage from washed beads. The complex was further purified by gel filtration on a Superdex 200 column in SEC buffer. Peak fractions were pooled and concentrated to 1 mg/mL for ATPase assays and cross-linking experiments.

1. Altschul SF, Gish W, Miller W, Myers EW, Lipman DJ (1990) Basic local alignment search tool. *J Mol Biol* 215(3):403–410.
2. ter Beek J, Duurkens RH, Erkens GB, Slotboom DJ (2011) Quaternary structure and functional unit of energy coupling factor (ECF)-type transporters. *J Biol Chem* 286(7): 5471–5475.
3. Bandrin SV, Rabinovich PM, Stepanov AI (1983) [3 linkage groups of the genes of riboflavin biosynthesis in Escherichia coli]. *Genetika* 19(9):1419–1425.
4. Zhang P, Wang J, Shi Y (2010) Structure and mechanism of the S component of a bacterial ECF transporter. *Nature* 468(7324):717–720.

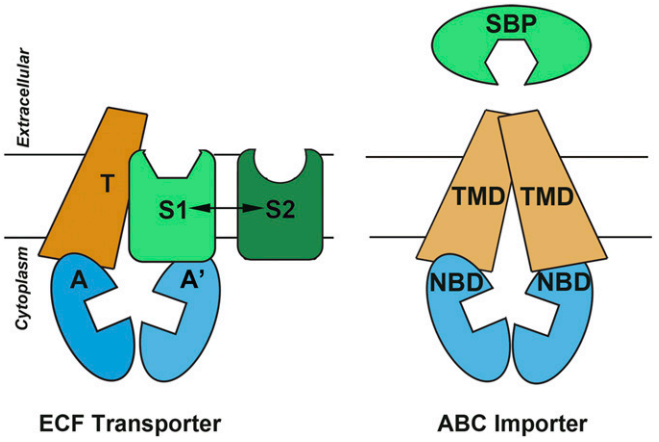

Fig. S1. Domain architecture of ECF transporters (*Left*) and ABC importers (*Right*). Both transporter families are powered by a pair of conserved ATPase domains, called A and A′ in ECF transporters and nucleotide binding domains (NBDs) or ABCs in ABC transporters. Group II ECF transporters use a transmembrane coupling protein (T) and multiple integral membrane substrate binding proteins (S). ABC importers possess a symmetrical architecture of two NBDs, two homologous transmembrane domains (TMDs), and a bilobed soluble substrate binding protein (SBP). The 1 × 4 subunit model for ECF transporters, in which the transporter is composed of one A, A′, T, and S (above) does not share this twofold symmetry.

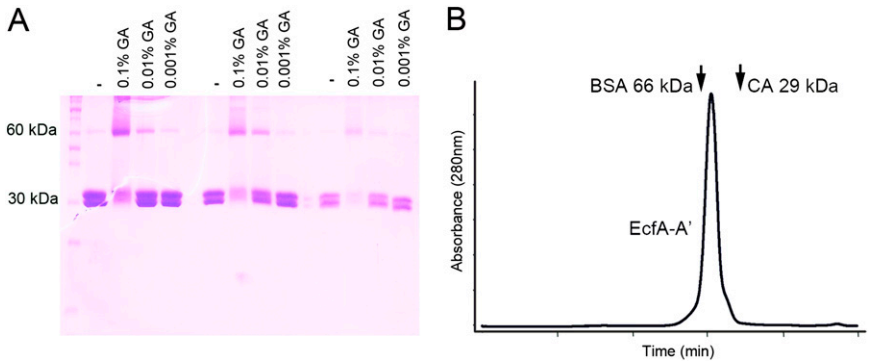

Fig. S2. The EcfA and A′ subunits heterodimerize in solution. (*A*) Glutaraldehyde (GA) cross-linking of the purified A and A′ complex at three protein concentrations leads to a dominant band at 60 kDa in all cases. (*B*) The oligomeric state of the complex was determined by comparison with the protein standards carbonic anhydrase (CA) and BSA (BSA) by SEC. The EcfA–A′ complex elutes at a position consistent with a 60 kDa heterodimer.

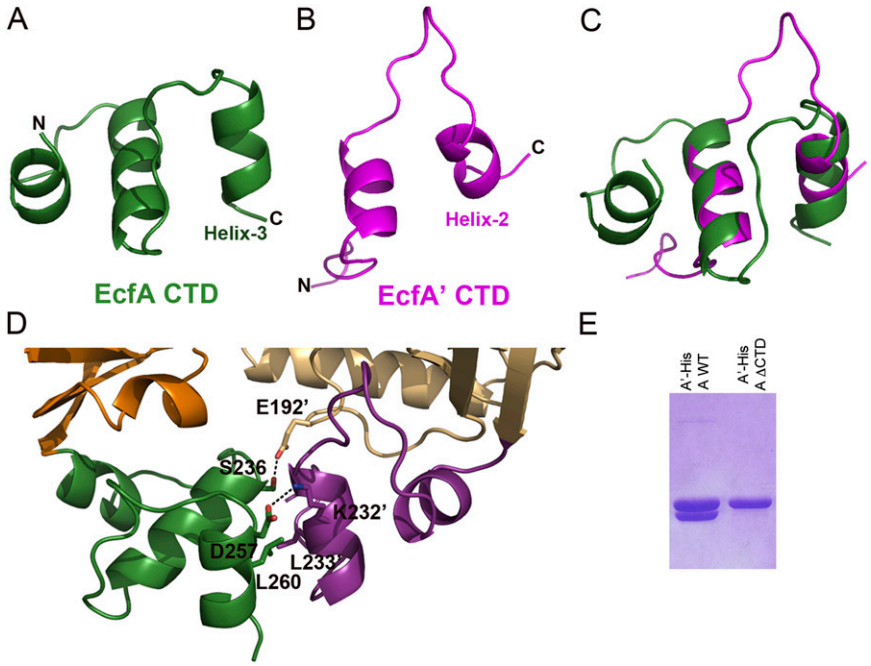

Fig. S3. The EcfA–A′ heterodimer associates via novel CTDs. (*A*) Structure of the EcfA CTD. (*B*) Structure of the EcfA′ CTD. (*C*) Superposition of the CTDs reveals a shared structure between the two helices of A′ and helices 2 and 3 of the A subunit but with an inverted orientation. (*D*) The CTDs interact primarily along helix-3 of the A subunit and helix-2 of A′. (*E*) Truncation of EcfA at Gly220 (A ΔCTD) removes the CTD and abolishes the copurification of the A–A′ heterodimer.

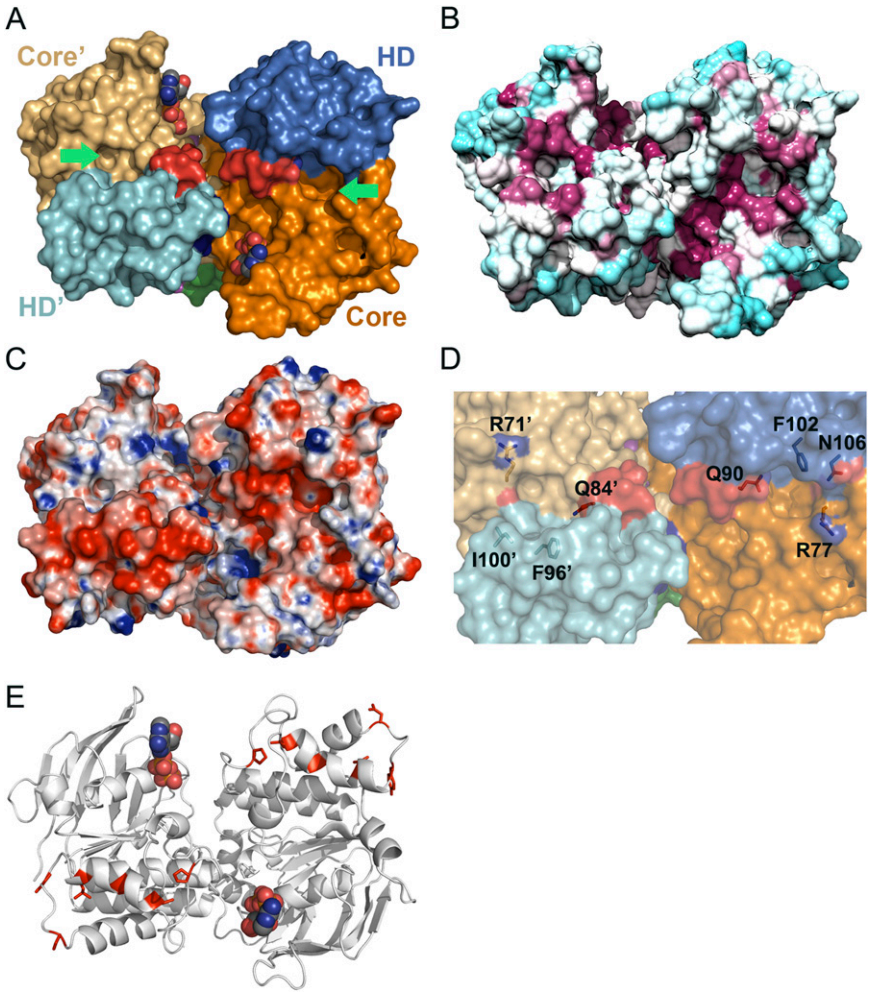

Fig. S4. Surface properties of the T-interaction site formed by the Q-helices in the EcfA–A′ heterodimer. (*A*) T-subunit facing surface of the A–A′ heterodimer colored by subdomain as in Fig. 3. The groove formed by the Q-helix and the helical subdomain in each subunit is indicated by the green arrows. (*B*) Sequence conservation of the same surface, where purple represents highly conserved and teal residues are variable. (*C*) Electrostatic surface potential reveals that the groove is negatively charged. (*D*) The groove is lined with conserved residues from the core subdomain (Arg77/71′), the first helix of the helical subdomain (Phe/96′ and Asn106/Ile100′), and the Q-helix (Gln90/84′). (*E*) Residues that could be cross-linked to the T subunit of the ECF biotin transporter are mapped onto the surface of the EcfA–A′ structure and colored red.

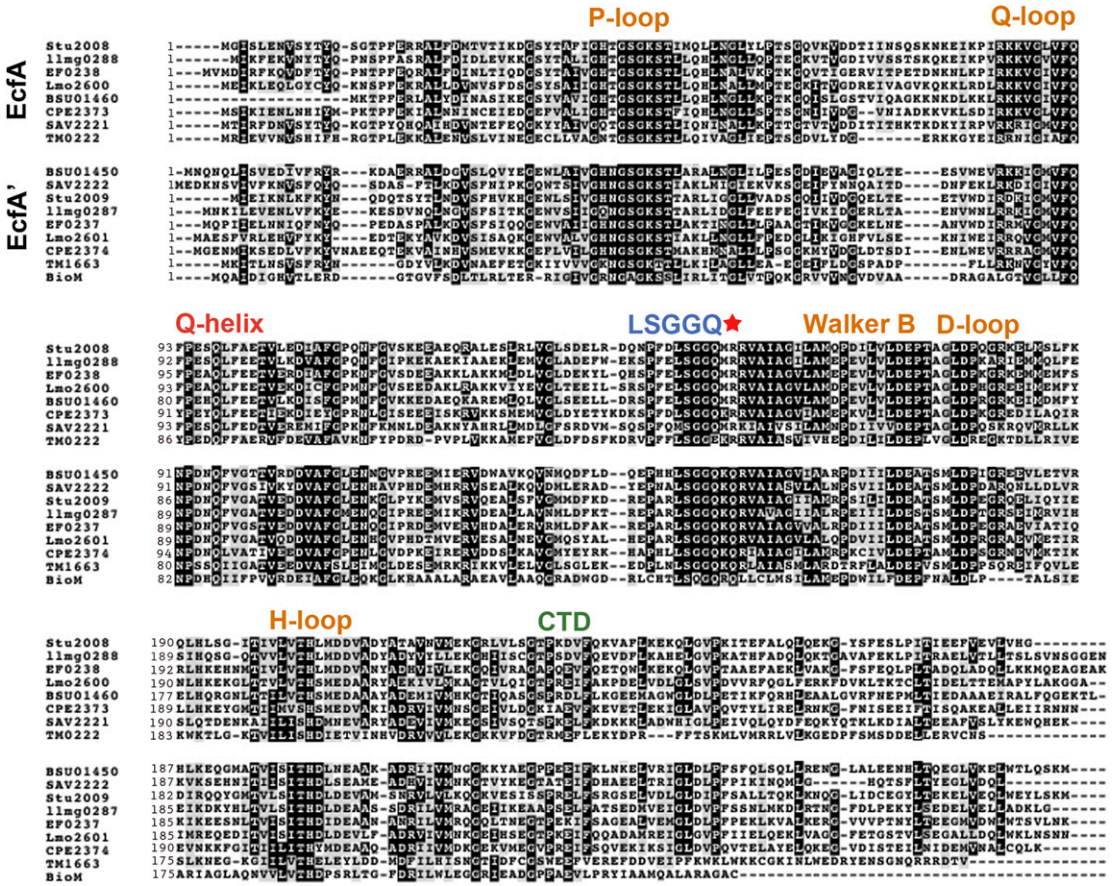

Fig. S5. Sequence conservation of ATPase subunits from ECF transporters. Sequence alignment of EcfA and A′ subunits from *S. thermophilus*, *L. lactis*, *Listeria monocytogenes*, *Bacillus subtilis*, *Staphylococcus aureus*, *Clostridium perfringes*, *Enterococcus faecalis*, *T. maritima*, and the BioM ATPase from the biotin ECF transporter from *Rhodobacter capsulatus*. Functionally important motifs are labeled and the residue that interacts with the Q-helix is marked with a red star.

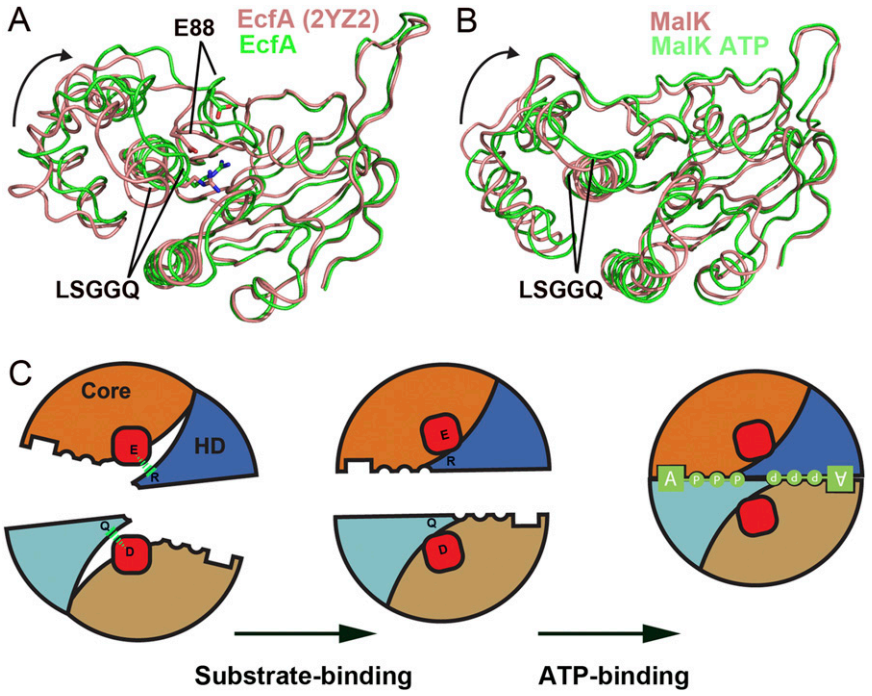

Fig. S6. Dynamic interactions between the Q-helix and the LSGGQ signature sequence. (*A*) Core domain superposition of EcfA subunits form the monomer (pink) and heterodimer structure (green). Loss of the salt bridge between Glu88 and Arg145 releases the helical domain, which assumes a conformation consistent with the ATP-bound state. (*B*) The core domain superposition of the MalK ATPase from the pretranslocation (pink) and ATP-bound (green) structures of the maltose transporter reveal a similar domain rotation. (*C*) Schematic illustrating how modulation of the interaction between the Q-helix and residues following the LSGGQ could play a role in coupling to the substrate-bound state of an ECF transporter.

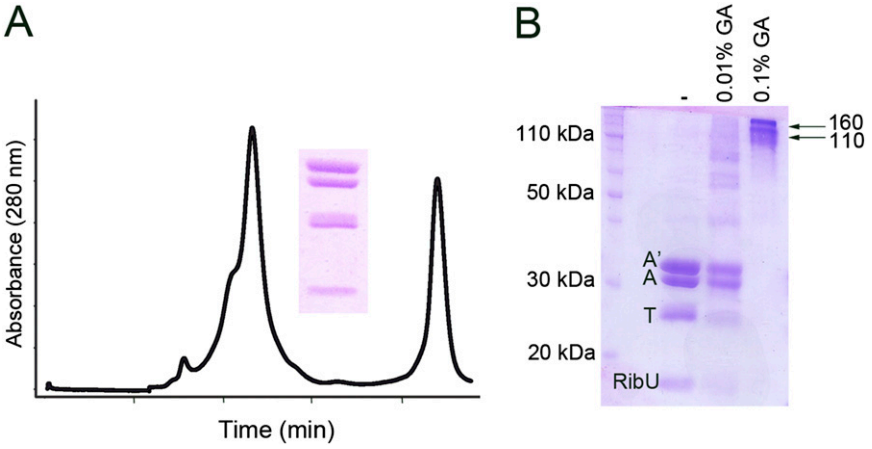

Fig. S7. Characterization of the ECF riboflavin transporter from *S. thermophilus*, StuECF–RibU. (*A*) SEC profile and SDS/PAGE (*Inset*) of purified StuECF–RibU. (*B*) Glutaraldehyde (GA) cross-linking of StuECF–RibU in detergent yields a dominant band at 160 kDa, consistent with a 3 × 2 subunit stoichiometry.

Table S1. Complementation of an *E. coli* riboflavin auxotroph by TmECF–RibU

	Riboflavin (mg/L)				
Genes	0	0.5	2.5	5	10
Vector	–	–	–	–	+
RibB	++	++	++	++	++
RibU (S)	–	–	–	–	+
T	–	–	–	–	+
A+A′	–	–	–	+	+
2 Vectors	–	–	–	+	+
RibU+A+A′	–	–	–	+	+
RibU+T	–	–	–	–	+
T+A+A′	–	–	–	+	+
RibU+T+A+A′	+	++	++	++	++

LB plates supplemented with the indicated amounts of riboflavin were scored as: –, no growth; +, slight growth 20–40 colonies; ++, strong growth 50–100 colonies.